TO THE EDITOR:

Primary resistance to CD19-directed chimeric antigen receptor T-cell therapy in T-cell/histiocyte-rich large B-cell lymphoma

Jonathan A. Trujillo,[1,*] James Godfrey,[1,2,*] Yifei Hu,[3,4] Jun Huang,[4] Sonali M. Smith,[1] Matthew J. Frigault,[5,6] Zachariah DeFilipp,[5,7] Daniel Appelbaum,[8] Yonglin Pu,[8] Nicholas Feinberg,[8] Thomas Althaus,[1,9] Michael R. Bishop,[1,9] Peter A. Riedell,[1,9] and Justin Kline[1,9]

[1]Section of Hematology/Oncology, Department of Medicine, The University of Chicago, Chicago, IL; [2]Department of Hematology and Hematopoietic Cell Transplantation, City of Hope, Duarte, CA; [3]Pritzker School of Medicine and [4]Pritzker School of Molecular Engineering, The University of Chicago, Chicago, IL; [5]Department of Medicine, [6]Cellular Immunotherapy Program, and [7]Blood and Marrow Transplant Program, Massachusetts General Hospital, Boston, MA; and [8]Department of Radiology and [9]David and Etta Jones Center for Cellular Therapy, The University of Chicago, Chicago, IL

We read with interest the recent report in *Blood* by Griffin et al,[1] which provided a detailed description of the topographical immune landscape of T-cell/histiocyte-rich large B-cell lymphoma (T/HRLBCL) and implicated the programmed cell death protein 1 (PD-1)/programmed cell death ligand 1 (PD-L1) pathway as a key driver of immune escape in this disease. T/HRLBCL is an uncommon variant of diffuse large B-cell lymphoma (DLBCL) that frequently presents at advanced stages with extranodal involvement in young to middle-aged men.[2] T/HRLBCL shares molecular and genomic characteristics with nodular lymphocyte-predominant Hodgkin lymphoma,[3,4] and the T/HRLBCL environment is also reminiscent of classical Hodgkin lymphoma. For instance, in contrast to most DLBCLs, which appear histologically as sheets of malignant B cells, T/HRLBCL is characterized by rare tumor cells scattered among a dense background of reactive T cells and macrophages (histiocytes).

A recent genetic and quantitative spatial analysis has provided important insights into the complex interactions occurring at the tumor-immune interface in T/HRLBCL.[1] Specifically, investigators identified recurrent *PD-L1* copy gains associated with high PD-L1 expression on malignant B cells often surrounded by an abundance of PD-L1–expressing macrophages and PD-1+ T cells. Interestingly, we have also identified a subset of DLBCLs similarly characterized by *PD-L1* gene alterations, an inflammatory microenvironment, and responsiveness to PD-1 blockade therapy.[5,6] It is therefore not surprising that 3 of 5 T/HRLBCL patients in the aforementioned study achieved objective responses to anti–PD-1 immunotherapy.[1] Collectively, these findings suggest that PD-L1 is a dominant immune checkpoint that mediates the dysfunction of endogenous T cells in T/HRLBCL.

The impact of the T/HRLBCL immune environment on the fate of adoptively transferred chimeric antigen receptor (CAR) T cells is not known. This question is highly relevant because, although CD19-directed CAR T-cell therapy has transformed the treatment of relapsed/refractory (r/r) DLBCL,[7,8] its efficacy in uncommon DLBCL subtypes, such as T/HRLBCL, is unknown, which represents a critical knowledge gap. Between July 2017 and December 2019, we identified 9 patients with r/r T/HRLBCL treated with axicabtagene ciloleucel (axi-cel) or tisagenlecleucel

(tisa-cel) CD19-directed CAR T-cell therapy at our institutions (patient tissue sections were obtained from institutional review board–approved institutional biorepositories in accordance with the Declaration of Helsinki). Seven patients received commercial CAR T-cell therapy, and 2 were treated on clinical trials of US Food and Drug Administration (FDA)-approved anti-CD19 CAR T cells for investigational indications. Patient characteristics are provided in Table 1. Patients were all male with a median age of 42 years and had received 1 to 5 prior treatments. CD19 expression was present on lymphoma cells in all evaluable pretreatment biopsies. Baseline metabolic tumor volume (MTV), serum lactate dehydrogenase, ferritin, and C-reactive protein were assessed in 7 of 9 patients (Table 1). Prior to CAR T-cell infusion, patients received lymphodepleting chemotherapy with FDA-recommended doses of fludarabine and cyclophosphamide. All patients were administered a single CAR T-cell infusion at a standard dose (axi-cel, 2×10^6 viable CAR+ T cells per kilogram; tisa-cel, 0.6-6.0×10^8 viable CAR+ T cells).

Cytokine release syndrome (CRS) occurred in all patients (grade 1-2), and immune effector cell-associated neurotoxicity syndrome (ICANS) was observed in 6 patients (grade 1-4), as assessed by American Society for Transplantation and Cellular Therapy (ASTCT) guidelines.[9] Five patients were administered tocilizumab and 2 received corticosteroids. Response assessments using positron emission tomography/computed tomography (PET/CT) imaging were performed between days 30 and 90 following CAR T-cell infusion. Remarkably, imaging demonstrated progressive disease by day 90 in all 9 patients. Eight of 9 patients had confirmatory biopsies. CD19 expression was maintained on lymphoma cells in all 5 assessable cases.

To investigate potential mechanisms underlying CAR T-cell therapy resistance, we performed a kinetic analysis of CAR T-cell expansion in the peripheral blood of 3 T/HRLBCL patients with available material. Here, we observed clear evidence of CAR T-cell expansion and contraction in a time-dependent manner (Figure 1A-B). Interestingly, PD-1 was highly coexpressed on a large proportion of circulating CAR T cells in all 3 patients, particularly at peak expansion (Figure 1A-B). These data suggest that failure of CAR T-cell therapy in T/HRLBCL is not likely due to poor

Table 1. Patient characteristics and outcomes following CAR T-cell therapy

Characteristics	Patient 1	Patient 2	Patient 3	Patient 4	Patient 5	Patient 6	Patient 7	Patient 8	Patient 9
Age, y	21	31	55	42	41	30	50	29	39
Sex	M	M	M	M	M	M	M	M	M
Disease stage	IVB	IVB	IVB	IVB	IVB	IVB	IVB	IVB	IVB
No. of prior therapies	2	4	3	3	5	2	5	1	2
Prior lines of therapy	1. R-EPOCH 2. R-GDP	1. R-EPOCH 2. R-ICE 3. R-Len 4. R-GEMOX	1. R-CHOP 2. R-ICE 3. R-GEMOX	1. R-CHOP 2. R-ICE 3. R-GEMOX	1. R-CHOP 2. R-ICE 3. ASCT 4. R-DHAP 5. R-Len	1. R-CHOP 2. R-ICE	1. R-CHOP 2. R-ICE 3. BV + Nivo 4. R-GEMOX 5. R-Len	1. R-CHOP + enzastaurin	1. R-CHOP 2. R-ICE
Disease status	Primary-refractory	Primary-refractory	Primary-refractory	Primary-refractory	Relapsed	Primary-refractory	Primary-refractory	Relapsed	Primary-refractory
Baseline (Ref. range)									
LDH, U/L (116-245 U/L)	872	509	343	577	342	293	*	141	*
CRP, mg/dL (<0.5 mg/dL)	2.8	4.3	7.9	12.4	0.7	0.5	*	0	*
Ferritin, ng/mL (20-300 ng/mL)	1578	242	1142	346	219	275	*	135	*
MTV, mL†	621.52	680.27	2160.83	1799.31	‡	711.1	1690	85.95	‡
ECOG PS	0	0	1	0	0	0	1	0	0
Bridging therapy	No	Yes	Yes	Yes	Yes	No	Yes	No	No
Product§	Axi-cel	Axi-cel	Axi-cel	Axi-cel	Axi-cel	Tisa-cel	Anti-CD19 CAR (clinical trial)	Anti-CD19 CAR (clinical trial)	Axi-cel
CRS	Grade 1	Grade 1	Grade 2	Grade 1	Grade 2	Grade 1	Grade 1	Grade 1	Grade 1

ASCT, autologous stem cell transplant; BV, brentuximab vedotin; CR, complete response; CRP, C-reactive protein; CRS, cytokine release syndrome; ECOG PS, Eastern Cooperative Oncology Group Performance Status; FC, flow cytometry; FISH, fluorescence in situ hybridization; ICANS, immune effector cell-associated neurotoxicity syndrome; LBCL, large B-cell lymphoma; LDH, lactate dehydrogenase; LN, lymph node; M, male; mIF, multispectral immunofluorescence; MTV, metabolic tumor volume; NA, not assessed; nivo, nivolumab; PD, progressive disease; Pembro, pembrolizumab; PET/CT, positron emission tomography/computed tomography; PR, partial response; R-CHOP, rituximab, cyclophosphamide, hydroxydaunorubicin, oncovin, prednisone; R-DHAP, rituximab, dexamethasone, ara-C, cisplatin; Ref., reference; R-EPOCH, rituximab, etoposide, prednisone, oncovin, cyclophosphamide, hydroxydaunorubicin; R-GDP, rituximab, gemcitabine, dexamethasone, cisplatin; R-GEMOX, rituximab, gemcitabine, oxaliplatin; R-ICE, rituximab, ifosfamide, carboplatin, etoposide; R-Len, rituximab, lenalidomide; RP, retroperitoneal.

*LDH, CRP, and ferritin levels unavailable.

†MTV indicates that whole-body metabolic tumor volume was ascertained from fluorodeoxyglucose (FDG)-PET/CT imaging.

‡PET/CT imaging unavailable for MTV calculation.

§Lymphodepleting chemotherapy regimen administered: patients 1 through 9 received fludarabine (30 mg/m² on days −5, −4, −3) and cyclophosphamide (500 mg/m² on days −5, −4, −3); patients 5 and 7 received fludarabine (25 mg/m² per day on days −5, −4, −3) and cyclophosphamide (250 mg/m² per day on days −5, −4, −3).

‖Patients 7 and 8 achieved PR at day 30 and subsequently progressed by day 60 and day 90, respectively. All other patients experienced disease progression at their first response assessment at the indicated time points.

¶NA denotes patients in whom CD19 expression on tumor tissue could not be assessed due to tissue exhaustion.

Table 1. (continued)

Characteristics	Patient 1	Patient 2	Patient 3	Patient 4	Patient 5	Patient 6	Patient 7	Patient 8	Patient 9
ICANS	Grade 1	Grade 1	Grade 2	Grade 1	Grade 4	Grade 0	Grade 2	Grade 0	Grade 0
Tocilizumab or steroids	No	Tocilizumab	Tocilizumab and steroids	Tocilizumab	Tocilizumab and steroids	No	No	Tocilizumab	No
Disease response assessment‖	PET/CT, day 60; PD	PET/CT, day 60; PD	PET/CT, day 30; PD	PET/CT, day 30; PD	PET/CT, day 30; PD	PET/CT, day 90; PD	PET/CT, day 60; PD	PET/CT, day 90; PD	PET/CT, day 30; PD
Response to CAR T-cell therapy	Refractory	Refractory	Refractory	Refractory	Refractory	Refractory	Refractory	Refractory	Refractory
Biopsy confirming relapse	LN biopsy, day 74: T/HRLBCL	RP mass, day 62: T/HRLBCL	Ascites, day 40: T/HRLBCL	Pleural fluid, day 34: LBCL	Bone marrow, day 125: T/HRLBCL	Not performed	Lung lesion, day 84: T/HRLBCL	Lung lesion, day 107: T/HRLBCL	RP mass, day 50: T/HRLBCL
CD19 expression									
Pre-CAR T¶	Yes	Yes	Yes	Yes	NA	Yes	Yes	Yes	Yes
Post-CAR T¶	Yes	Yes	Yes	Yes	Yes	NA	NA	NA	NA
Response to subsequent anti–PD-1 therapy	Pembro, PD	Pembro, PD				Pembro, ongoing CR		Nivo, PR	Pembro, PD
Survival status	Alive	Deceased	Deceased	Deceased	Deceased	Alive	Deceased	Alive	Deceased
Assays performed	mIF PD-L1 FISH: disomic	mIF PD-L1 FISH: disomic		FC	FC mIF, posttreatment	FC PD-L1 FISH: amplified	mIF PD-L1 FISH: disomic		

ASCT, autologous stem cell transplant; BV, brentuximab vedotin; CR, complete response; CRP, C-reactive protein; CRS, cytokine release syndrome; LBCL, large B-cell lymphoma; LDH, lactate dehydrogenase; LN, lymph node; M, male; mIF, multispectral immunofluorescence; MTV, metabolic tumor volume; NA, not assessed; nivo, nivolumab; PD, progressive disease; Pembro, pembrolizumab; PET/CT, positron emission tomography/computed tomography; PR, partial response; R-CHOP, rituximab, cyclophosphamide, hydroxydaunorubicin, oncovin, prednisone; R-DHAP, rituximab, dexamethasone, ara-C, cisplatin; Ref., reference; R-EPOCH, rituximab, etoposide, prednisone, oncovin, cyclophosphamide, hydroxydaunorubicin; R-GDP, rituximab, gemcitabine, dexamethasone, cisplatin; R-GEMOX, rituximab, gemcitabine, oxaliplatin; R-ICE, rituximab, ifosfamide, carboplatin, etoposide; R-Len, rituximab, lenalidomide; RP, retroperitoneal.

*LDH, CRP, and ferritin levels unavailable.

†MTV indicates that whole-body metabolic tumor volume was ascertained from fluorodeoxyglucose (FDG)-PET/CT imaging.

‡PET/CT imaging unavailable for MTV calculation.

§Lymphodepleting chemotherapy regimen administered: patients 1 through 9 received fludarabine (30 mg/m² on days −5, −4, −3) and cyclophosphamide (500 mg/m² on days −5, −4, −3); patient 6 received fludarabine (25 mg/m² per day on days −5, −4, −3) and cyclophosphamide (250 mg/m² per day on days −5, −4, −3).

‖Patients 7 and 8 achieved PR at day 30 and subsequently progressed by day 60 and day 90, respectively. All other patients experienced disease progression at their first response assessment at the indicated time points.

¶NA denotes patients in whom CD19 expression on tumor tissue could not be assessed due to tissue exhaustion.
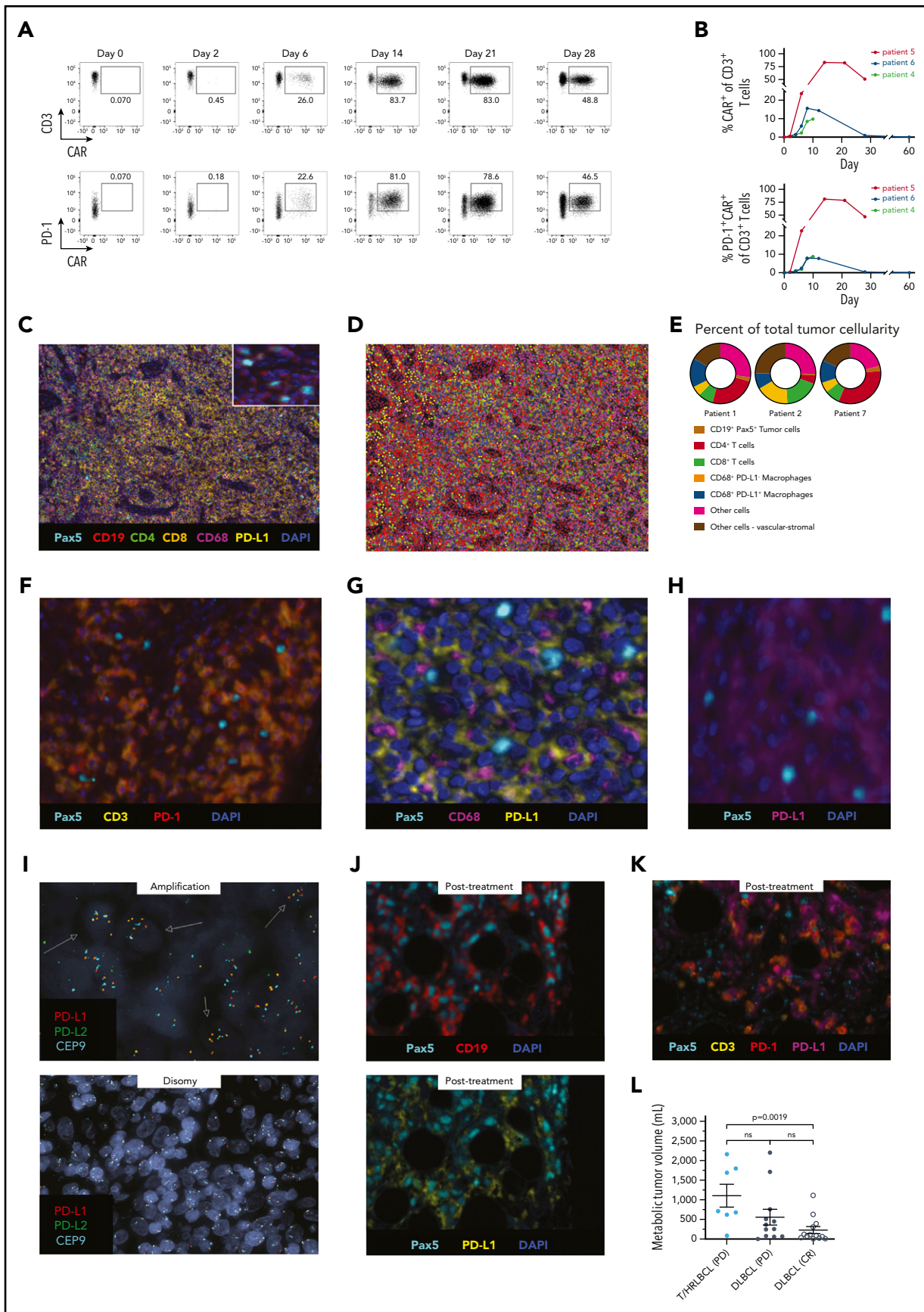
LETTER TO *BLOOD*

Figure 1.

CAR T-cell expansion, and argue that other factors, such as acquired CAR T-cell dysfunction, could be responsible for the poor clinical outcomes observed.

Given the striking PD-1 expression on CAR T cells described herein, the extent and cellular distribution of PD-L1 expression in the T/HRLBCL environment was defined through multispectral immunofluorescence (mIF) microscopy on 3 available pretreatment biopsies. As shown in Figure 1C, mIF analysis revealed strong CD19 expression on Pax5+ lymphoma cells, as well as a prominent T-cell and macrophage infiltrate (Figure 1C-E). Numerous PD-1+ T cells were also identified in close proximity to lymphoma cells throughout the tumor microenvironment (Figure 1F). PD-L1 expression was particularly abundant on CD68+ macrophages that were often juxtaposed to sparsely distributed lymphoma cells, which also expressed PD-L1 (Figure 1G-H). PD-L1 fluorescence in situ hybridization (FISH) demonstrated PD-L1 gene amplification in 1 of 4 T/HRLBCL cases (Figure 1I). At the time of lymphoma progression following CAR T-cell therapy, tissue was available for mIF analysis in 1 T/HRLBCL case. Here, lymphoma-involved bone marrow showed preserved CD19 expression on malignant B cells that were PD-L1+ (Figure 1J) and surrounded by numerous PD-1–expressing T cells (Figure 1K). Given these findings, 5 T/HRLBCL patients were treated with anti–PD-1 therapy following CAR T-cell progression, and 2 achieved objective responses, including the patient with a PD-L1 gene amplification (Table 1).

In conclusion, we report that r/r T/HRLBCL is highly resistant to CD19-directed CAR T-cell therapy. This observation is striking, as reported response rates to CAR T-cell therapy in r/r DLBCL are as high as 83%.[8] Therefore, we believe our findings represent a true signal of inherent CAR T-cell resistance in T/HRLBCL, likely owing to the unique immune environment that defines this disease. Indeed, consistent with a recent publication,[1] we observed ubiquitous expression of PD-L1 on tumor-associated macrophages, PD-L1 gene alterations within malignant B cells, and robust PD-1 expression among T cells in the T/HRLBCL environment. Moreover, we identified striking PD-1 upregulation on peripheral blood CAR T cells from T/HRLBCL patients over time. Thus, it is interesting to speculate that PD-1/PD-L1 interactions not only promote the dysfunction of endogenous tumor-reactive T cells in T/HRLBCL as previously suggested,[1] but may also contribute to CAR T-cell resistance by inhibiting the function of adoptively transferred CAR T cells. However, as this study is limited by sample size, patient heterogeneity, and limited assessment of specimens following CAR T-cell therapy progression, our results should be considered hypothesis-generating.

For instance, we cannot entirely rule out CD19 antigen loss as a contributor to CAR T-cell therapy failure, as CD19 expression was not assessed in all T/HRLBCL cases at progression. However, CD19 loss is uncommon among lymphomas progressing early after CAR T-cell therapy, as was the case in our patients. High disease burden has also been linked with axi-cel CAR T-cell therapy failure in DLBCL,[10] and, interestingly, the mean baseline MTV in T/HRLBCL patients included in this study (n = 7) was higher than that of DLBCL patients (n = 13) who achieved durable responses to CAR T-cell therapy at The University of Chicago (Figure 1L). Although not all T/HRLBCL patients exhibited high baseline MTV, disease burden may have also contributed to CAR T-cell therapy failure in a fraction of cases. Despite the noted limitations of this study, our observations are nevertheless important in alerting physicians to the preliminarily

Figure 1. In vivo CAR T-cell expansion kinetics in T/HRLBCL patients and multispectral immune profiling of the T/HRLBCL microenvironment. (A) Representative flow cytometry plots showing frequencies of peripheral blood CAR+CD3+ cells (top panels) and of PD-1+CAR+CD3+ cells (bottom panels; gated on CD3+ cells) prior to and at the indicated time points following CAR T-cell infusion. PBMCs were stained with anti-CD3 antibody, anti-PD-1 antibody, and anti-CAR antibody (clone Y45). (B) Quantitative data depicting CAR+CD3+ T-cell frequencies in peripheral blood of 3 T/HRLBCL patients prior to and at the indicated time points following CAR T-cell therapy (top panel), and frequencies of PD-1+CAR+CD3+ T cells in peripheral blood prior to and at the indicated time points following CAR T-cell therapy (bottom panel). (C) Representative mIF image of a pretreatment T/HRLBCL specimen demonstrating scattered malignant B cells surrounded by numerous PD-L1+ macrophages and T cells. Representative merged mIF staining for Pax5 (light blue), CD19 (red), CD4 (light green), CD8 (orange), CD68 (magenta), PD-L1 (yellow), and nuclear 4′,6-diamidino-2-phenylindole (DAPI) counterstain (blue). Overlaying high-power image of Pax5 (light blue) and CD19 (red) staining showing CD19 expression by Pax5+ lymphoma cells. Images were captured using the Vectra Polaris imaging platform and Phenochart software (PerkinElmer). Image analysis and the generation of cell phenotype maps were performed using a supervised machine learning algorithm within the Inform 2.3 software (PerkinElmer), which assigned trained phenotypes and Cartesian coordinates to cells. mIF staining performed using primary antibodies (anti-Pax5 [BC/24, BioCare Medical], anti-CD19 [CD19, BioCare Medical], anti-CD4 [4B12, BioCare Medical], anti-CD8 [C8/144B, R&D], anti-CD68 [KP1, BioCare Medical], anti-PD-L1 [E1L3N, Cell Signaling] detected with horseradish-peroxidase (HRP)-conjugated secondary antibodies and Opal fluorophores; original magnification ×20. (D) Cell phenotype maps corresponding to the mIF image in panel C were used to determine immune cell composition and location. Each cell type is represented by a color-coded dot as indicated in the key in panel E. Original magnification × 20. (E) Wheel chart showing the percentage of each cell subset per total number of nucleated cells in each T/HRLBCL tumor specimen pre-CAR T-cell therapy. Colors for each cell type coincide with colored dots in the phenotype map. (F) High-power view of mIF staining for Pax5 (light blue), CD3 (yellow), and PD-1 (red) demonstrating PD-1 expression on the surface of CD3+ T cells in the T/HRLBCL microenvironment prior to CAR T-cell therapy. mIF staining performed using primary antibodies (anti-Pax5, anti-CD3 [EP41, BioCare Medical], anti-PD-1 [EPR4877, Abcam]) detected with HRP-conjugated secondary antibodies and Opal fluorophores; original magnification ×85. (G) Representative staining for Pax5 (light blue), CD68 (magenta), and PD-L1 (yellow) demonstrating Pax5+ lymphoma cells surrounded by numerous PD-L1–expressing CD68+ macrophages prior to CAR T-cell therapy. mIF staining performed using primary antibodies (anti-Pax5, anti-CD68, anti-PD-L1) detected with HRP-conjugated secondary antibodies and Opal fluorophores; original magnification ×100. (H) High-power view of Pax5 (light blue) and PD-L1 (magenta) staining demonstrating PD-L1 expression by Pax5+ lymphoma cells. mIF staining performed using primary antibodies (anti-Pax5, anti-PD-L1) detected with HRP-conjugated secondary antibodies and Opal fluorophores; original magnification ×100. (I) PD-L1 FISH images from a T/HRLBCL case with PD-L1/PD-L2 gene amplification (top panel) and a separate PD-L1/PD-L2 disomic T/HRLBCL case (bottom panel). Arrows indicate representative lymphoma cells harboring increased copy numbers (>2) of PD-L1 (orange signal) and PD-L2 (light green signal) compared with the centromere 9 control (light blue signal) FISH probes. FISH probes targeted PD-L1 (red signal) [CD274, Empire Genomics], region centromeric to PD-L1 (light green signal) [RP11-610G2, Empire Genomics] and centromere 9 (light blue signal) [CEP9, Abbott]; nuclei stained with DAPI; original magnification ×100. (J) Representative mIF image of bone marrow tissue exhibiting lymphoma involvement at the time of disease progression after CAR T-cell therapy demonstrating CD19 (red; top panel) and PD-L1 (yellow; bottom panel) expression by Pax5+ lymphoma cells (light blue). mIF staining performed using primary antibodies (anti-Pax5, anti-CD19, anti-PD-L1) detected with HRP-conjugated secondary antibodies and Opal fluorophores; original magnification ×40. (K) High-power view of mIF staining for Pax5 (light blue), CD3 (yellow), PD-1 (red), and PD-L1 (magenta) revealing PD-1+ T cells in close proximity to Pax5+ lymphoma cells and PD-L1+ cells in the bone marrow of a patient with disease progression after CAR T-cell therapy. mIF staining performed using primary antibodies (anti-Pax5, anti-CD3, anti-PD-1, anti-PD-L1) detected with HRP-conjugated secondary antibodies and Opal fluorophores; original magnification ×40. (L) Baseline MTV, derived from PET/CT imaging, in T/HRLBCL and DLBCL patients treated with CAR T-cell therapy at The University of Chicago. MTV data are reported as mean plus or minus standard error of the mean (SEM); 2-tailed, unpaired Student t test. CR, DLBCL patients achieving durable complete remission following CAR T-cell therapy; ns, not significant; PD, patients with progressive disease following CAR T-cell therapy.

LETTER TO *BLOOD*

poor activity of CAR T-cell therapy in T/HRLBCL, and in stimulating the exploration of alternative treatments, such as PD-1 blockade therapy, in this disease.

Acknowledgments

Authorship

Contribution: J.A.T. and J.G. collected patient data, procured biopsy specimens, performed data analysis, and wrote the manuscript; M.J.F., Z.D., T.A., M.R.B., and P.A.R. contributed patient data and reviewed the manuscript; J.K. conceived the project, contributed patient data, and contributed to drafting and reviewing the manuscript; S.M.S. reviewed the manuscript; Y.H. and J.H. performed analyses for in vivo CAR T-cell expansion; and D.A., Y.P., and N.F. conducted all MTV analyses.

Conflict-of-interest disclosure: S.M.S. has served as a consultant for Morphosys/Incyte, Janssen, Bristol Myers Squibb (BMS), Karyopharm, TG Therapeutics (TGTX), and Celgene, and has received research funding from FortySeven, TGTX, Pharmacyclics, Acerta, Karyopharm, Portola, Celgene, Novartis, Genentech/Roche, and Epizyme. M.J.F. has served on advisory boards or provided consulting to Novartis, Celgene/BMS, Kite/Gilead, and Arcellx. Z.D. receives research support from Incyte and Regimmune, and has received consulting fees from Syndax Pharmaceuticals. M.R.B. receives research support from Kite/Gilead, Novartis, Arcellx, and CRISPR Therapeutics; has served on advisory boards for Kite/Gilead, Novartis, Arcellx, CRISPR Therapeutics, Autolus, Juno, and Celgene; and has served on speakers' bureaus for BMS, Incyte, Sanfi, and Kite/Gilead. P.A.R. receives research support from Kite/Gilead, Novartis, Celgene/BMS, MorphoSys, and Calibr; has served on advisory boards for or provided consulting to Bayer, Novartis, Kite/Gilead, Karyopharm, Verastem, and Celgene/BMS; and has served on speakers' bureaus for Bayer and Kite/Gilead. J.K. receives research support from Merck, Verastem, and iTeos; has served on a speaker's bureau for Kite/Gilead; and has served on advisory boards for Verastem, Seattle Genetics, MorphoSys, and Karyopharm. The remaining authors declare no competing financial interests.

ORCID profiles: J.A.T., 0000-0002-0184-9773; J.G., 0000-0002-4103-4288; Y.H., 0000-0003-2870-7772; J.H., 0000-0003-0271-4384; S.M.S., 0000-0002-9893-4949; Z.D., 0000-0002-7994-8974; Y.P., 0000-0002-9583-8185; P.A.R., 0000-0003-2719-0580.

Correspondence: Justin Kline, Section of Hematology/Oncology, Department of Medicine, The University of Chicago, 900 East 57th St, Chicago, IL 60637; e-mail: jkline@medicine.bsd.uchicago.edu.

Footnotes

REFERENCES

1. Griffin GK, Weirather JL, Roemer M, et al. Spatial signatures identify immune escape via PD-1 as a defining feature of T-cell/histiocyte-rich large B-cell lymphoma [published online ahead of print 1 September 2020]. *Blood.* doi:10.1182/blood.2020006464.

2. Ollila TA, Reagan JL, Olszewski AJ. Clinical features and survival of patients with T-cell/histiocyte-rich large B-cell lymphoma: analysis of the National Cancer Data Base. *Leuk Lymphoma.* 2019;60(14):3426-3433.

3. Schuhmacher B, Bein J, Rausch T, et al. JUNB, DUSP2, SGK1, SOCS1 and CREBBP are frequently mutated in T-cell/histiocyte-rich large B-cell lymphoma. *Haematologica.* 2019;104(2):330-337.

4. Pittaluga S, Jaffe ES. T-cell/histiocyte-rich large B-cell lymphoma. *Haematologica.* 2010;95(3):352-356.

5. Godfrey J, Tumuluru S, Bao R, et al. PD-L1 gene alterations identify a subset of diffuse large B-cell lymphoma harboring a T-cell-inflamed phenotype. *Blood.* 2019;133(21):2279-2290.

6. Kline J, Godfrey J, Ansell SM. The immune landscape and response to immune checkpoint blockade therapy in lymphoma. *Blood.* 2020;135(8):523-533.

7. Schuster SJ, Bishop MR, Tam CS, et al; JULIET Investigators. Tisagenlecleucel in adult relapsed or refractory diffuse large B-cell lymphoma. *N Engl J Med.* 2019;380(1):45-56.

8. Locke FL, Ghobadi A, Jacobson CA, et al. Long-term safety and activity of axicabtagene ciloleucel in refractory large B-cell lymphoma (ZUMA-1): a single-arm, multicentre, phase 1-2 trial. *Lancet Oncol.* 2019;20(1):31-42.

9. Lee DW, Santomasso BD, Locke FL, et al. ASTCT consensus grading for cytokine release syndrome and neurologic toxicity associated with immune effector cells. *Biol Blood Marrow Transplant.* 2019;25(4):625-638.

10. Dean EA, Mhaskar RS, Lu H, et al. High metabolic tumor volume is associated with decreased efficacy of axicabtagene ciloleucel in large B-cell lymphoma. *Blood Adv.* 2020;4(14):3268-3276.